

A luminous, blue progenitor system for a type-Iax supernova

Curtis McCully¹, Saurabh W. Jha¹, Ryan J. Foley^{2,3}, Lars Bildsten^{4,5},
Wen-fai Fong⁶, Robert P. Kirshner⁶, G. H. Marion^{7,6}, Adam G. Riess^{8,9},
& Maximilian D. Stritzinger¹⁰

August 7, 2014

authors' version, accepted to *Nature*; final version available at <http://dx.doi.org/10.1038/nature13615>

¹Department of Physics and Astronomy, Rutgers, the State University of New Jersey, 136 Frelinghuysen Road, Piscataway, New Jersey 08854, USA. ²Astronomy Department, University of Illinois at Urbana-Champaign, 1002 W. Green Street, Urbana, Illinois 61801, USA. ³Department of Physics, University of Illinois at Urbana-Champaign, 1110 W. Green Street, Urbana, Illinois 61801, USA. ⁴Department of Physics, University of California, Santa Barbara, California 93106, USA. ⁵Kavli Institute for Theoretical Physics, University of California, Santa Barbara, California 93106, USA. ⁶Harvard-Smithsonian Center for Astrophysics, 60 Garden Street, Cambridge, Massachusetts 02138, USA. ⁷Department of Astronomy, University of Texas at Austin, Austin, Texas 78712, USA. ⁸Department of Physics and Astronomy, Johns Hopkins University, 3400 North Charles Street, Baltimore, Maryland 21218, USA. ⁹Space Telescope Science Institute, 3700 San Martin Drive, Baltimore, Maryland 21218, USA. ¹⁰Department of Physics and Astronomy, Aarhus University, Ny Munkegade 120, DK-8000 Aarhus C, Denmark.

Type-Iax supernovae (SN Iax) are stellar explosions that are spectroscopically similar to some type-Ia supernovae (SN Ia) at maximum light, except with lower ejecta velocities^{1,2}. They are also distinguished by lower luminosities. At late times, their spectroscopic properties diverge from other SN³⁻⁶, but their composition (dominated by iron-group and intermediate-mass elements^{1,7}) suggests a physical connection to normal SN Ia. These are not rare; SN Iax occur at a rate between 5 and 30% of the normal SN Ia rate¹. The leading models for SN Iax are thermonuclear explosions of accreting carbon-oxygen white dwarfs (C/O WD) that do not completely unbind the star⁸⁻¹⁰, implying they are “less successful” cousins of normal SN Ia, where complete disruption is observed. Here we report the detection of the luminous, blue progenitor system of the type-Iax SN 2012Z in deep pre-explosion imaging. Its luminosity, colors, environment, and similarity to the progenitor of the Galactic helium nova V445 Puppi¹¹⁻¹³, suggest that SN 2012Z was the explosion of a WD accreting from a helium-star companion. Observations in the next few years, after SN 2012Z has faded, could test this hypothesis, or alternatively show that this supernova was actually the explosive death of a massive star^{14,15}.

SN 2012Z was discovered¹⁶ in the Lick Observatory Supernova Search on UT 2012-Jan-29.15. It had an optical spectrum similar to the type-Iax (previously called SN 2002cx-like) SN 2005hk³⁻⁵ (see Extended Data Fig. 1). The similarities between SN Iax and normal SN Ia make understanding SN Iax progenitors important, especially because no normal SN Ia progenitor has been identified. Like core-collapse SN (but also slowly-declining, luminous SN Ia), SN Iax are found preferentially in young, star-forming galaxies^{17,18}. A single SN Iax, SN 2008ge, was in a relatively old (S0) galaxy with no indication of current star formation to deep limits¹⁹. Non-detection of the progenitor of SN 2008ge in *Hubble Space Telescope (HST)* pre-explosion imaging restricts its initial mass $\lesssim 12 M_{\odot}$, and combined with the lack of hydrogen or helium in the SN 2008ge spectrum, favours a white dwarf progenitor¹⁹.

Deep observations of NGC 1309, the host galaxy of SN 2012Z, were obtained with *HST* in 2005–2006 and 2010, serendipitously including the location of the supernova before its explosion. To pinpoint the position of SN 2012Z with high precision, we obtained follow-up *HST* data in 2013. Colour-composite images made from these observations before and after the supernova are shown in Fig. 1, and photometry of stellar sources in the pre-explosion images near the supernova location is reported in Extended Data Table 1. We detect a source, called S1, coincident with the supernova at a formal separation of $0''.0082 \pm 0''.0103$ (equal to 1.3 ± 1.6 pc at 33 Mpc, the distance to NGC 1309^{20,21}). The pre-explosion data reach a 3σ limiting magnitude of $M_V \approx -3.5$, quite deep for typical extragalactic SN progenitor searches²², but certainly the possibility exists that the progenitor system of SN 2012Z was of lower luminosity and would be undetected in our data (as has been the case for all normal SN Ia progenitor searches to date²³). However, the locations of SN 2012Z and S1 are identical to within 0.8σ , and we estimate only a 0.24% (2.1%) probability that a random position near SN 2012Z would be within 1σ (3σ) of any detected star, making a chance alignment unlikely (see Methods, and Extended Data Fig. 2). We also observe evidence for vari-

ability in S1 (plausible for a pre-supernova system; Extended Data Table 2), at a level exhibited by only 4% of objects of similar brightness. We thus conclude there is a high likelihood that S1 is the progenitor system of SN 2012Z.

The color-magnitude diagram (CMD) presented in Fig. 2 shows S1 to be luminous and blue, yet in an odd place for a star about to explode. If its light is dominated by a single star, S1 is moderately consistent with a $\approx 18.5 M_{\odot}$ main-sequence star²⁴, an $\approx 11 M_{\odot}$ blue supergiant early in its evolution off the main sequence, or perhaps a $\approx 7.5 M_{\odot}$ (initial mass) blue supergiant later in its evolution (with core helium-burning in a blue loop, where models are quite sensitive to metallicity and rotation²⁵). None of these stars are expected to explode in standard stellar evolution theory, particularly without any signature of hydrogen in the supernova²².

The SN 2012Z progenitor system S1 is in a similar region in the CMD to some Wolf-Rayet stars²⁶, highly evolved, massive stars, that are expected to undergo core collapse and may produce a supernova. If S1 were a single Wolf-Rayet star, its photometry is most consistent with the WN subtype and an initial mass $\approx 30\text{--}40 M_{\odot}$, thought perhaps to explode with a helium-dominated outer layer as a SN Ib²⁷, and unlikely to produce the structure and composition of ejecta seen in SN Iax^{1,3,6,7}. Moreover, isochrones²⁴ fit to the neighbouring stars (Extended Data Fig. 3) yield an age range of $\approx 10\text{--}42$ Myr, longer than the 5–8 Myr lifetime of such a massive Wolf-Rayet star.

S1 may be dominated by accretion luminosity; its brightness in B and V is not far from the predicted thermal emission of an Eddington-luminosity Chandrasekhar mass WD (a super-soft source; SSS; Fig. 2). However, its V-I and V-H colours are too red for a SSS model. A composite scenario, with accretion power dominating the blue flux, and another source providing the redder light (perhaps a fainter, red donor star) may be plausible.

The leading models of SN Iax^{8–10} are based on C/O WD explosions, so S1 may be the companion star to an accreting WD. Although there are a variety of potential progenitor systems (including main-sequence and red giant donors, which are inconsistent with S1 if they dominate the system’s luminosity), in standard scenarios no companion star can have an initial mass greater than $\approx 7 M_{\odot}$; otherwise, there would not be enough time to form the primary C/O WD that explodes. Thus, the photometry of S1 suggests that if it is the companion to a C/O WD, recent binary mass transfer must have played a role in its evolution. One model for a luminous, blue companion star is a relatively massive ($\approx 2 M_{\odot}$ when observed) helium star^{11,28,29}, formed after binary mass transfer and a common envelope phase (e.g., a close binary with initial masses ≈ 7 and $4 M_{\odot}$). Although the model parameter space has not been fully explored, the predicted region for helium star donors in a binary system with a $1.2 M_{\odot}$ initial-mass accreting C/O WD²⁹ in the CMD is shown in Fig. 2, and S1 is consistent with being in this region. The evolutionary timescale for such a model is also well-matched to the ages of nearby stars (Extended Data Fig. 3).

SN 2012Z and the star S1 have an interesting analogue in our own Milky Way Galaxy: the helium nova V445 Pup^{11–13},

thought to be the surface explosion of a near-Chandrasekhar mass helium-accreting WD. Though S1 is somewhat brighter than the pre-explosion observations of V445 Pup, their consistent colours, similar variability amplitude¹³, and the physical connection between V445 Pup and likely SN Iax progenitors^{8–10} is highly suggestive. Indeed, two SN Iax (though not SN 2012Z itself) have shown evidence for helium in the system^{1,17}. In this model, a low helium accretion rate could lead to a helium nova (like V445 Pup), whereas a higher mass-transfer rate could result in stable helium burning on the C/O WD, allowing it to grow in mass before the supernova. The accretion is expected to begin as the helium star starts to evolve and grow in radius; indeed, the S1 photometry is consistent with the evolutionary track of a helium star with a mass (after losing its hydrogen envelope) of $\approx 2 M_{\odot}$, on its way to becoming a red giant¹¹.

Though the scenario of a helium-star donor to an exploding carbon-oxygen white dwarf is a promising model for the progenitor and supernova observations, we cannot yet rule out the possibility that S1 is a single star that itself exploded. Fortunately, by late 2015, SN 2012Z will have faded below the brightness of S1, and *HST* imaging will allow us to distinguish these models. Our favoured interpretation of S1 as the companion star predicts that it will still be detected (though perhaps modified by the impact of its exploding neighbour, a reduction in accretion luminosity, or a cessation of variability). On the other hand, if S1 has completely disappeared, it will be a strong challenge to models of SN Iax, and perhaps significantly blur the line between thermonuclear white-dwarf supernovae and massive-star core-collapse supernovae, with important impacts to our understanding of stellar evolution and chemical enrichment.

1. Foley, R. J. *et al.* Type Iax Supernovae: A New Class of Stellar Explosion. *Astrophys. J.* **767**, 57 (2013).
2. Li, W. *et al.* SN 2002cx: The Most Peculiar Known Type Ia Supernova. *Publ. Astron. Soc. Pacif.* **115**, 453–473 (2003).
3. Jha, S. *et al.* Late-Time Spectroscopy of SN 2002cx: The Prototype of a New Subclass of Type Ia Supernovae. *Astron. J.* **132**, 189–196 (2006).
4. Phillips, M. M. *et al.* The Peculiar SN 2005hk: Do Some Type Ia Supernovae Explode as Deflagrations? *Publ. Astron. Soc. Pacif.* **119**, 360–387 (2007).
5. Sahu, D. K. *et al.* The Evolution of the Peculiar Type Ia Supernova SN 2005hk over 400 Days. *Astrophys. J.* **680**, 580–592 (2008).
6. McCully, C. *et al.* Hubble Space Telescope and Ground-based Observations of the Type Iax Supernovae SN 2005hk and SN 2008A. *Astrophys. J.* **786**, 134 (2014).
7. Stritzinger, M. D. *et al.* Optical and near-IR observations of the faint and fast 2008ha-like supernova 2010ae. *Astron. Astrophys.* **561**, A146 (2014).
8. Jordan, G. C., IV, Perets, H. B., Fisher, R. T. & van Rossum, D. R. Failed-detonation Supernovae: Subluminous Low-velocity Ia Supernovae and their Kicked Remnant White Dwarfs with Iron-rich Cores. *Astrophys. J.* **761**, L23 (2012).
9. Kromer, M. *et al.* 3D deflagration simulations leaving bound remnants: a model for 2002cx-like Type Ia supernovae. *Mon. Not. R. Astron. Soc.* **429**, 2287–2297 (2013).
10. Fink, M. *et al.* Three-dimensional pure deflagration models with nucleosynthesis and synthetic observables for Type Ia supernovae. *Mon. Not. R. Astron. Soc.* **438**, 1762–1783 (2014).

11. Kato, M., Hachisu, I., Kiyota, S. & Saio, H. Helium Nova on a Very Massive White Dwarf: A Revised Light-Curve Model of V445 Puppis (2000). *Astrophys. J.* **684**, 1366–1373 (2008).
12. Woudt, P. A. *et al.* The Expanding Bipolar Shell of the Helium Nova V445 Puppis. *Astrophys. J.* **706**, 738–746 (2009).
13. Goranskij, V., Shugarov, S., Zharova, A., Kroll, P. & Barsukova, E. A. The Progenitor and Remnant of the Helium Nova V445 Puppis. *Pere-mennye Zvezdy* **30**, 4 (2010).
14. Valenti, S. *et al.* A low-energy core-collapse supernova without a hydrogen envelope. *Nature* **459**, 674–677 (2009).
15. Moriya, T. *et al.* Fallback Supernovae: A Possible Origin of Peculiar Supernovae with Extremely Low Explosion Energies. *Astrophys. J.* **719**, 1445–1453 (2010).
16. Cenko, S. B. *et al.* Supernova 2012Z in NGC 1309 = Psn J03220535-1523156. *Central Bureau Electronic Telegrams* **3014**, 1 (2012).
17. Foley, R. J. *et al.* SN 2008ha: An Extremely Low Luminosity and Exceptionally Low Energy Supernova. *Astron. J.* **138**, 376–391 (2009).
18. Lyman, J. D. *et al.* Environment-derived constraints on the progenitors of low-luminosity Type I supernovae. *Mon. Not. R. Astron. Soc.* **434**, 527–541 (2013).
19. Foley, R. J. *et al.* On the Progenitor and Supernova of the SN 2002cx-like Supernova 2008ge. *Astron. J.* **140**, 1321–1328 (2010).
20. Riess, A. G. *et al.* Cepheid Calibrations of Modern Type Ia Supernovae: Implications for the Hubble Constant. *Astrophys. J. Suppl. Ser.* **183**, 109–141 (2009).
21. Riess, A. G. *et al.* A 3% Solution: Determination of the Hubble Constant with the Hubble Space Telescope and Wide Field Camera 3. *Astrophys. J.* **730**, 119 (2011).
22. Smartt, S. J. Progenitors of Core-Collapse Supernovae. *Annu. Rev. Astron. Astrophys.* **47**, 63–106 (2009).
23. Li, W. *et al.* Exclusion of a luminous red giant as a companion star to the progenitor of supernova SN 2011fe. *Nature* **480**, 348–350 (2011).
24. Bertelli, G., Nasi, E., Girardi, L. & Marigo, P. Scaled solar tracks and isochrones in a large region of the Z-Y plane. II. From 2.5 to 20 M_{\odot} stars. *Astron. Astrophys.* **508**, 355–369 (2009).
25. Georgy, C. *et al.* Populations of rotating stars. I. Models from 1.7 to 15 M at $Z = 0.014, 0.006,$ and 0.002 with $\Omega/\Omega_{\text{crit}}$ between 0 and 1. *Astron. Astrophys.* **553**, A24 (2013).
26. Shara, M. M. *et al.* The Vast Population of Wolf-Rayet and Red Supergiant Stars in M101. I. Motivation and First Results. *Astron. J.* **146**, 162 (2013).
27. Groh, J. H., Meynet, G., Georgy, C. & Ekström, S. Fundamental properties of core-collapse supernova and GRB progenitors: predicting the look of massive stars before death. *Astron. Astrophys.* **558**, A131 (2013).
28. Iben, I., Jr. & Tutukov, A. V. Helium star cataclysmics. *Astrophys. J.* **370**, 615–629 (1991).
29. Liu, W.-M., Chen, W.-C., Wang, B. & Han, Z. W. Helium-star evolutionary channel to super-Chandrasekhar mass type Ia supernovae. *Astron. Astrophys.* **523**, A3 (2010).

Acknowledgments Supernova 2012Z was discovered just weeks after the passing of our dear friend and colleague, Weidong Li, whose work on the Lick Observatory Supernova Search, SN 2002cx-like supernovae, and Hubble Space Telescope observations of SN progenitors, continues to inspire us. That those three foci of Weidong’s research converge here in this paper makes our hearts glad, and we dedicate this paper to his memory.

We thank the SH₀ES team for assistance with data from *HST* program GO-12880, E. Bertin for the development of the STIFF software to produce color images, and A. Dolphin for software and guidance in photometry. This research at Rutgers University was supported through NASA/*HST* grant GO-12913.01, and National Science Foundation (NSF) CAREER award AST-0847157 to S.W.J. NASA/*HST* grant GO-12999.01 to R.J.F. supported this work at the University of Illinois. At UC Santa Barbara, this work was supported

by NSF grants PHY 11-25915 and AST 11-09174 to L.B. The Danish Agency for Science, Technology, and Innovation supported M.D.S. through a Sapere Aude Level 2 grant.

Support for *HST* programs GO-12913 and GO-12999 was provided by NASA through a grant from the Space Telescope Science Institute, which is operated by the Association of Universities for Research in Astronomy, Incorporated, under NASA contract NAS5-26555.

Author Contributions C.M., S.W.J., and R.J.F. performed the data analysis and were chiefly responsible for preparing the manuscript and figures. W.F., R.P.K., G.H.M., and A.G.R. assisted in developing the proposal to obtain *HST* observations, including acquiring supporting ground-based photometry and spectroscopy. L.B. provided insight into models for progenitor systems. M.D.S. analyzed ground-based photometry and spectroscopy of the supernova, used as input for this paper. All authors contributed to extensive discussions about, and edits to, the paper draft.

Competing Interests The authors declare that they have no competing financial interests.

Correspondence Correspondence and requests for materials should be addressed to S.W.J. (saurabh@physics.rutgers.edu).

Methods

Observations and reduction. SN 2012Z provides a unique opportunity to search for a SN Iax progenitor, because of deep, pre-explosion *HST* observations. Its face-on spiral host galaxy NGC 1309 was also the site of the nearby, normal type-Ia SN 2002fk, and as such was targeted in 2005 and 2006 with the *HST* Advanced Camera for Surveys (ACS) and in 2010 with the *HST* Wide-Field Camera 3 (WFC3) optical (UVIS) and infrared (IR) channels, to observe Cepheid variable stars in order to anchor the SN Ia distance scale (*HST* programs GO-10497, GO-10802, and GO-11570, PI: A. Riess; GO/DD-10711, PI: K. Noll). To measure the location of SN 2012Z with high precision, we used *HST* WFC3/UVIS images of NGC 1309 (fortuitously including SN 2012Z) taken on UT 2013-Jan-04 (program GO-12880; PI: A. Riess), as well as targeted *HST* WFC3/UVIS images of SN 2012Z taken on UT 2013-Jun-30 (GO-12913; PI: S. Jha).

The 2005–2006 ACS images include 2 visits totaling 9600s of exposure time in the F435W filter (similar to Johnson *B*), 14 visits for a total exposure of 61760 sec in F555W (close to Johnson *V*) and 5 visits for 24000s in F814W (analogous to Cousins *I*). These are showing the blue, green, and red channels, respectively of panels a–c in Fig. 1. We re-reduced the archived data, combining the multiple exposures (including sub-sampling and cosmic ray rejection) using the AstroDrizzle software from the DrizzlePac package³⁰, with the results shown in panels b and c of Fig. 1. The bottom right panels d and e of Fig. 1 show our combined *HST* WFC3/UVIS F555W (blue; 1836 sec) + F625W (green; 562 sec) + F814W (red; 1836 sec) images from January and June 2013, with SN 2012Z visible.

We used the DrizzlePac TweakReg routine to register all of the individual flatfielded (“`flt`”) frames to the WFC3/UVIS F555W image taken on UT 2013-Jan-04. The typical root-mean-square (rms) residual of individual stars from the relative astrometric solution was $0''.009$, corresponding to 0.18 pixels in ACS and 0.23 pixels in WFC3/UVIS. We drizzle the ACS images to the native scale of UVIS, $0''.04$ per pixel (20% smaller than the native $0''.05$ ACS pixels) and subsample the ACS point-spread function (psf) correspondingly with a pixel fraction parameter of 0.8.

Photometry and astrometry. In Extended Data Table 1, we present photometry of sources in the region based on the *HST* ACS images from 2005–2006 (F435W, F555W, and F814W), as well as WFC3/IR F160W data (6991 sec of total exposure time) from 2010. The stars are sorted by their proximity to the SN position, and their astrometry is referenced to SDSS images of the field, with an absolute astrometric uncertainty of $0''.080$ (but this is irrelevant for the much more precise relative astrometry of SN 2012Z and S1). We photometered the *HST* images using the psf-fitting software DolPhot, an extension of HSTPhot³¹. We combined individual fit frames taken during the same *HST* visit at the same position, and then used DolPhot to measure photometry using recommended parameters for ACS and WFC3.

The WFC3/UVIS images of SN 2012Z from January and June 2013 provide a precise position for the supernova of R.A. = $3^{\text{h}}22^{\text{m}}05^{\text{s}}.39641$, Decl. = $-15^{\circ}23'14''.9390$ (J2000) with a

registration uncertainty of $0''.0090$ (plus an absolute astrometric uncertainty of $0''.08$, irrelevant to the relative astrometry). As shown in Fig. 1 we detect a stellar source (called S1) in the pre-explosion images coincident with the position of the SN with a formal separation, including centroid uncertainties, of $0''.0082 \pm 0''.0103$, indicating an excellent match and strong evidence for S1 being the progenitor system of SN 2012Z.

Chance alignment probability. To estimate the probability of a chance alignment, we use the observed density of sources detected with signal-to-noise ratio $S/N > 3.0$ (in any filter) and $S/N > 3.5$ (in all bands combined, via DolPhot) in a 200×200 pixel ($8'' \times 8''$) box centered on SN 2012Z (452 sources), and find only a 0.24% (2.1%) chance that a random position would be consistent with a detected star at 1σ (3σ). Moreover, only 171 of these stars are as bright as S1, so *a posteriori* there was only a 0.09% (0.80%) chance of a 1σ (3σ) alignment with such a bright object. As shown in Extended Data Fig. 2, these results are not especially sensitive to the size of the region used to estimate the density of sources, at least down to 50×50 pixels ($2'' \times 2''$) around SN 2012Z. Nearer than this, the density of sources increases by a factor of a few, though with substantially larger uncertainty given the low number of sources (including S1 itself). We base our fiducial chance alignment probability on the larger region where the density of sources stabilizes with good statistics, but our qualitative results do not depend on this choice.

Given the surface brightness of NGC 1309, we crudely estimate $\approx 160 M_{\odot}$ in stars projected within an area corresponding to our 1σ error circle ($\approx 8 \text{ pc}^2$). These should be roughly uniformly distributed throughout this small region, so our chance alignment probability should accurately quantify the probability that SN 2012Z originated from an undetected progenitor that was only coincidentally near a detected source like S1.

The pre-explosion data for SN 2012Z are the deepest ever for a SN Iax, reaching $M_V \approx -3.5$; the next best limits come from SN 2008ge¹⁹, which yielded no progenitor detection down to $M_V \approx -7$. The star S1, at $M_V \approx -5.3$, would not have been detected in any previous search for SN Iax progenitors. This implies that our chance alignment probability calculation can be taken at face value; there have not been previous, unsuccessful “trials” that would reduce the unlikelihood of a chance coincidence. Viewed in the context of progenitor searches for normal SN Ia, in only two cases: SN 2011fe²³ and SN 2014J³², would a star of the luminosity of S1 have been clearly detected in pre-explosion data. Other normal SN Ia, like SN 2006dd³³, have progenitor detection limits in pre-explosion observations just near, or above, the luminosity of S1.

Variability of S1. NGC 1309 was imaged over 14 epochs in F555W with ACS before SN 2012Z exploded. Examining these individually, we find some evidence for variability in S1; the photometry is presented in Extended Data Table 2. Formally, these data rule out the null hypothesis of no variability at 99.95% (3.5σ), with $\chi^2 = 36.658$ in 13 degrees of freedom. However, most of the signal is driven by one data point (MJD 53600.0; a 4.2σ outlier); excluding this data point (though we find no independent reason to do so) reduces the significance of the vari-

ability to just 91.1% (1.7σ). To empirically assess the likelihood of variability, we looked to see how often stars with the same brightness as S1 (within 0.5 mag) doubled in brightness relative to their median like S1 in one or more of the 14 epochs; we find that just 4% do so (4 of the nearest 100, 9 of the nearest 200, and 20 of nearest 500 such stars). As variability might be expected in a SN progenitor before explosion (from non-uniform accretion, for example), combining this with the chance alignment probability strengthens the identification of S1 as the progenitor system of SN 2012Z. It also disfavours the possibility that S1 is a compact, unresolved star cluster.

Properties of S1 and nearby stars. In Fig. 2 we present colour-magnitude diagrams of S1 and other objects for comparison. In the figure, S1 has been corrected for Milky Way reddening ($E(B-V)_{MW} = 0.035$ mag, corresponding to $A_{F435W} = 0.14$ mag, $A_{F555W} = 0.11$ mag, $A_{F814W} = 0.06$ mag), and host reddening ($E(B-V)_{host} = 0.07$ mag; $A_{F435W} = 0.28$ mag, $A_{F555W} = 0.22$ mag, $A_{F814W} = 0.12$ mag) based on narrow, interstellar absorption lines in high-resolution spectroscopy of SN 2012Z itself³⁴. This low extinction is consistent with the photometry and spectroscopy of SN 2012Z, as well as its location in the outskirts of a face-on spiral host. For the potential Galactic analogue V445 Puppis progenitor, we correct its photometry for Galactic and circumstellar reddening¹².

Fig. 2 also shows stellar evolution tracks²⁴ for stars with initial masses of 7, 8, 9, 10, and 11 M_{\odot} , adopting a metallicity of 0.87 solar, based on the H II region metallicity gradient²⁰ for NGC 1309 interpolated to the SN radial location. The Eddington-luminosity accreting Chandrasekhar-mass white dwarfs are shown as the large purple dots, with each subsequent dot representing a change in temperature of 1000 K. These “super-soft” sources are fainter in F555W for higher temperatures (and bluer F435W–F555W colours) as the fixed (Eddington-limited) bolometric luminosity emerges in the ultraviolet for hotter systems. The shaded blue region represents the range of helium-star donors for C/O WD SN progenitor models starting with a 1.2 M_{\odot} white dwarf²⁹. We converted the model temperatures and luminosities to our observed bands assuming a blackbody spectrum. The expected temperature and luminosity for this class of models is expected to vary with white dwarf mass, and therefore, we regard this region as approximate; its shape, size, and location is subject to change.

S1 is inconsistent with all confirmed progenitors of core-collapse SN (exclusively SN II), which are mostly red supergiants²². The blue supergiant progenitor of, e.g., SN 1987A, was significantly more luminous and likely more massive than S1³⁵. However, we caution that our theoretical expectations for massive stars could be modified if S1 is in a close binary system where mass transfer has occurred.

The stars detected in the vicinity of S1 provide clues to the nature of recent star formation in the region. They include red supergiants (like S2 and S3 from Table 1) as well as objects bluer and more luminous than S1 (like S5). We show CMDs including these stars in Extended Data Fig. 3; the stars plotted have a signal-to-noise ratio $S/N > 3.5$ in the displayed filters, and were required to be no closer than 3 pixels to a brighter source to avoid

photometric uncertainties from crowding. Model isochrones²⁴ imply that these stars span an age range of ≈ 10 –42 Myr. These tracks favour an initial mass for S1 of ≈ 7 –8 M_{\odot} (neglecting mass transfer) if it is roughly coeval with its neighbours. In other words, if S1 were a 30–40 M_{\odot} initial-mass Wolf-Rayet star with a predicted lifetime of only 5–8 Myr²⁷, it would be the youngest star in the region.

30. Gonzaga, S., Hack, W., Fruchter, A. & Mack, J. *The DrizzlePac Handbook* (STScI, Baltimore, 2012).
31. Dolphin, A. E. WFPC2 Stellar Photometry with HSTPHOT. *Publ. Astron. Soc. Pacif.* **112**, 1383–1396 (2000).
32. Kelly, P. L. *et al.* Constraints on the Progenitor System of the Type Ia Supernova 2014J from Pre-explosion Hubble Space Telescope Imaging. *Astrophys. J.* **790**, 3 (2014).
33. Maoz, D. & Mannucci, F. A search for the progenitors of two Type Ia Supernovae in NGC 1316. *Mon. Not. R. Astron. Soc.* **388**, 421–428 (2008).
34. Stritzinger, M. D. *et al.* Comprehensive Observations of the Bright and Energetic Type Iax SN 2012Z: Interpretation as a Chandrasekhar Mass White Dwarf Explosion. *Astron. Astrophys.* (2014, submitted).
35. Arnett, W. D., Bahcall, J. N., Kirshner, R. P. & Woosley, S. E. Supernova 1987A. *Annu. Rev. Astron. Astrophys.* **27**, 629–700 (1989).

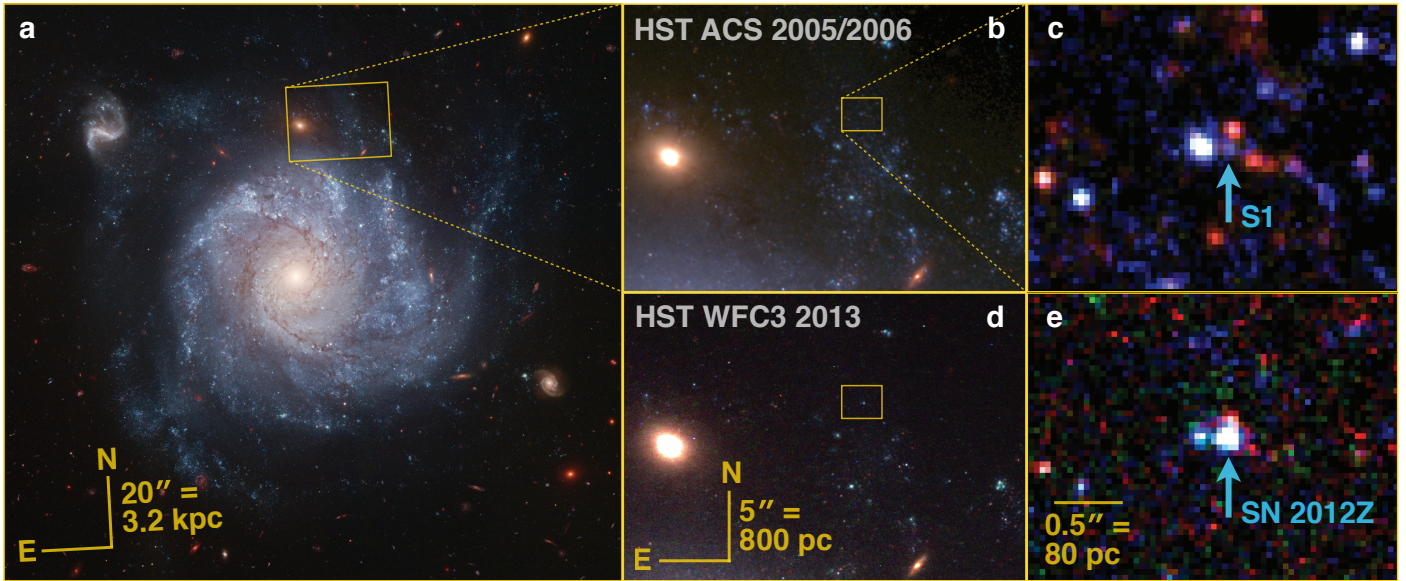


Figure 1 | *Hubble Space Telescope* colour images before and after supernova 2012Z. Panel a shows the Hubble Heritage image of NGC 1309 (<http://heritage.stsci.edu/2006/07>), with panels b and c zooming in on the progenitor system S1 in the deep, pre-explosion data. Lower panels d and e show the shallower post-explosion images of SN 2012Z on the same scale as the panels above.

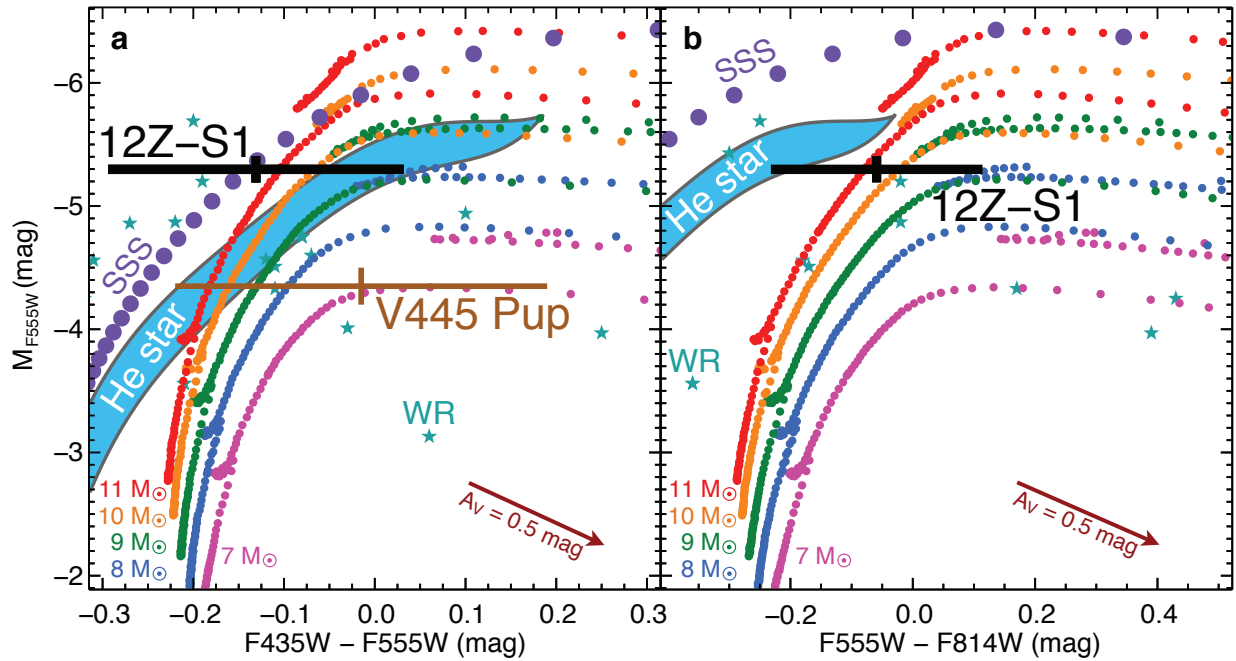
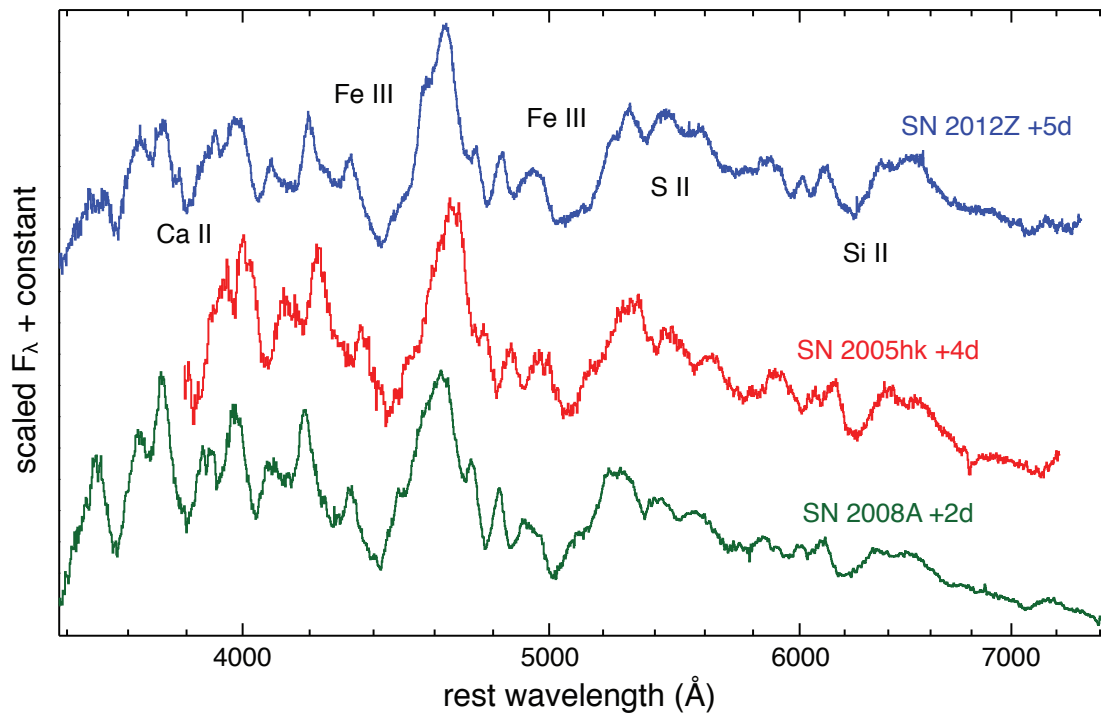
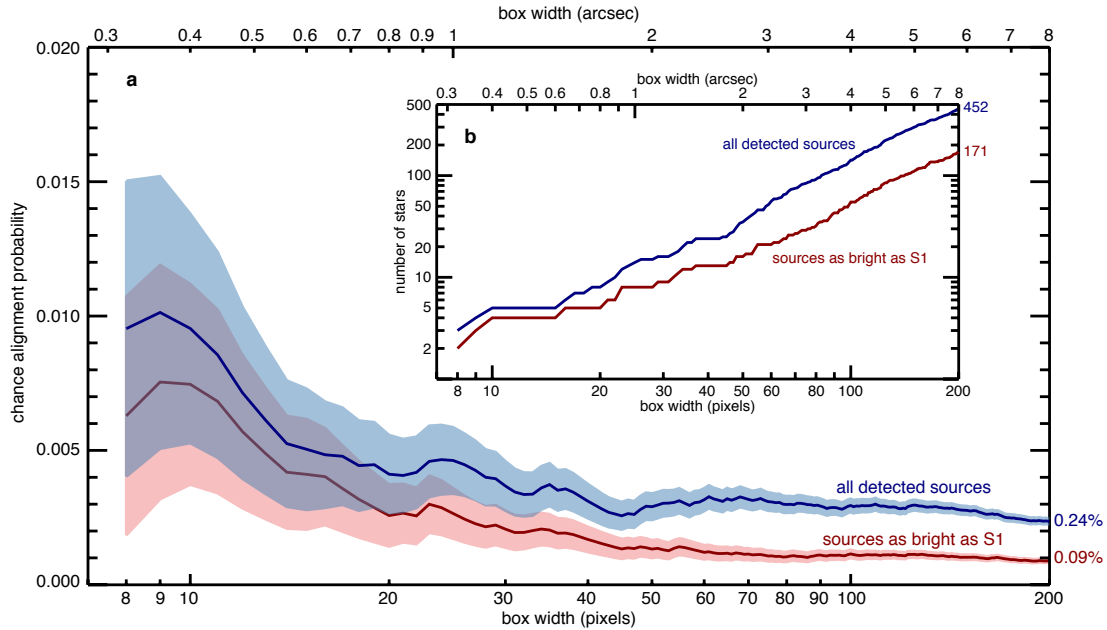


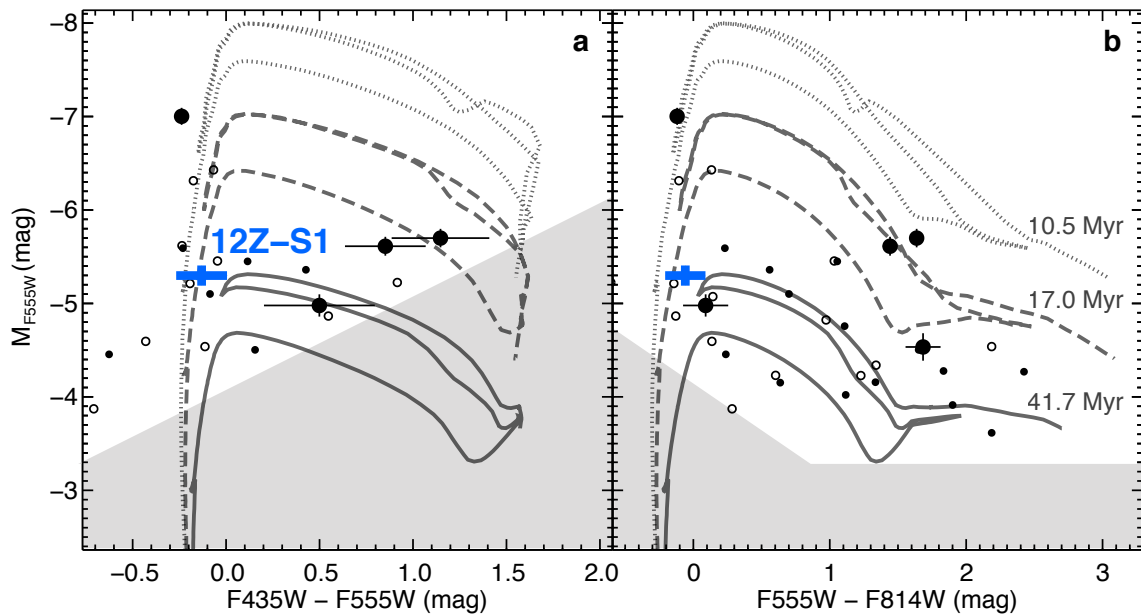
Figure 2 | Colour-magnitude diagrams of the SN 2012Z progenitor system S1 and comparison models. Panel a presents the F435W-F555W colour (roughly B-V), while panel b shows F555W-F814W (V-I), both plotted against the F555W (V) absolute magnitude. The black and brown crosses represent the progenitor systems for SN 2012Z and V445 Puppis¹², respectively, with 1σ photometric uncertainties. Other comparisons plotted include evolutionary tracks²⁴ for single stars (coloured dotted curves), thermal models for Eddington-luminosity super-soft sources (SSS; purple dots), candidate Wolf-Rayet stars²⁶ (blue-gray stars), and models for helium-star donors to $1.2 M_{\odot}$ initial mass C/O WDs²⁹ (shaded blue regions).



Extended Data Figure 1 | Spectra of SN Iax near maximum light. SN 2012Z¹ is similar to SN 2005hk⁴ and SN 2008A⁶, all classified as SN Iax. The SN 2012Z spectrum was taken on UT 2012-02-16 with the Whipple Observatory 1.5m telescope (+FAST spectrograph) with a total exposure time of 1800 sec. Each spectrum is labelled by its rest-frame phase past *B* maximum light. Prominent features due to intermediate-mass and iron group elements are indicated; these features are also observed in luminous, slowly-declining SN Ia spectra at maximum light, though with higher expansion velocities.



Extended Data Figure 2 | Chance alignment probability calculation. Panel a shows the chance alignment probability between a random position and a detected source within a square box of the given width centered at the position of SN 2012Z. This calculation is based on a 1σ position coincidence ($0''.0103 = 0.2575$ WFC3/UVIS pixels); a 3σ position coincidence gives probabilities approximately 9 times higher. The offset between SN 2012Z and S1 is 0.8σ . The shaded regions show a naive Poisson-like uncertainty estimate with a fractional error given by $1/\sqrt{N_{\text{sources}}}$. Panel b shows the number of detected sources (including S1) as a function of the box size. The lines show results for all stellar sources ($>3\sigma$ detection in any band; blue) and just those as bright as S1 (red).



Extended Data Figure 3 | Stars in the neighbourhood of the SN 2012Z progenitor. The SN 2012Z progenitor system S1 (blue) is shown along with nearby stars (all with 1σ photometric uncertainties), with three isochrones²⁴ with ages of 10.5 (dotted), 17.0 (dashed), and 41.7 Myr (solid). Panel a presents the F435W-F555W colour (roughly B-V), while panel b shows F555W-F814W (V-I), both plotted against the F555W (V) absolute magnitude. The large, filled circles correspond to stars within 10 WFC3/UVIS pixels ($0''.4$) of the SN location, small filled circles are within 20 pixels ($0''.8$), and the small open circles are within 30 pixels ($1''.2$). Objects in the gray shaded regions would not be detected given the depth of the combined images.

Extended Data Table 1 | Pre-explosion photometry of SN 2012Z progenitor system S1 and nearby stars. The 1σ photometric uncertainty is given in parentheses and non-detections are listed with 3σ upper-limits. No corrections for Galactic or host extinction are made here.

Star	R.A. (J2000)	Decl. (J2000)	F435W (mag)	F555W (mag)	F814W (mag)	F160W (mag)
S1	3 ^h 22 ^m 05 ^s .39591	-15° 23' 14." 9350	27.589 (0.122)	27.622 (0.060)	27.532 (0.135)	26.443 (0.321)
S2	3 ^h 22 ^m 05 ^s .40280	-15° 23' 14." 9402	>29.221	28.551 (0.116)	27.463 (0.093)	26.032 (0.238)
S3	3 ^h 22 ^m 05 ^s .39483	-15° 23' 14." 8102	28.466 (0.258)	27.221 (0.041)	25.435 (0.022)	23.699 (0.027)
S4	3 ^h 22 ^m 05 ^s .38460	-15° 23' 15." 0314	28.258 (0.211)	27.308 (0.046)	25.717 (0.028)	23.887 (0.033)
S5	3 ^h 22 ^m 05 ^s .41013	-15° 23' 14." 9362	25.778 (0.029)	25.918 (0.014)	25.888 (0.030)	25.435 (0.136)
S6	3 ^h 22 ^m 05 ^s .37564	-15° 23' 15." 0702	>28.807	28.386 (0.116)	26.553 (0.055)	24.986 (0.085)
S7	3 ^h 22 ^m 05 ^s .41970	-15° 23' 14." 8454	28.539 (0.286)	27.942 (0.078)	27.703 (0.146)	26.436 (0.322)
S8	3 ^h 22 ^m 05 ^s .37049	-15° 23' 14." 6690	>28.847	28.763 (0.164)	27.279 (0.101)	25.032 (0.092)
S9	3 ^h 22 ^m 05 ^s .36477	-15° 23' 15." 0634	27.683 (0.127)	27.470 (0.050)	26.266 (0.042)	24.753 (0.069)
S10	3 ^h 22 ^m 05 ^s .39605	-15° 23' 15." 4062	>28.912	29.305 (0.273)	26.969 (0.077)	25.214 (0.102)
S11	3 ^h 22 ^m 05 ^s .37904	-15° 23' 14." 5218	27.196 (0.083)	27.329 (0.045)	26.949 (0.076)	>26.614
S12	3 ^h 22 ^m 05 ^s .37556	-15° 23' 14." 4202	>28.897	28.302 (0.109)	27.095 (0.085)	25.381 (0.131)
S13	3 ^h 22 ^m 05 ^s .36527	-15° 23' 14." 5054	28.085 (0.181)	27.560 (0.055)	26.852 (0.069)	25.740 (0.171)
S14	3 ^h 22 ^m 05 ^s .40432	-15° 23' 15." 5778	>29.360	28.651 (0.113)	26.078 (0.026)	24.180 (0.042)
S15	3 ^h 22 ^m 05 ^s .43040	-15° 23' 14." 4706	27.937 (0.164)	28.465 (0.122)	28.078 (0.208)	>26.512
S16	3 ^h 22 ^m 05 ^s .42376	-15° 23' 14." 3726	>28.765	28.163 (0.092)	26.905 (0.072)	25.126 (0.094)
S17	3 ^h 22 ^m 05 ^s .38194	-15° 23' 14." 2494	>28.926	29.007 (0.207)	26.957 (0.077)	26.230 (0.260)
S18	3 ^h 22 ^m 05 ^s .35086	-15° 23' 15." 2402	27.831 (0.143)	27.819 (0.069)	26.969 (0.077)	25.581 (0.145)
S19	3 ^h 22 ^m 05 ^s .39387	-15° 23' 14." 2018	28.670 (0.302)	28.417 (0.118)	26.616 (0.056)	25.072 (0.094)
S20	3 ^h 22 ^m 05 ^s .37179	-15° 23' 15." 6186	>28.814	28.643 (0.147)	26.660 (0.059)	24.854 (0.075)
S21	3 ^h 22 ^m 05 ^s .34566	-15° 23' 15." 4618	>28.813	>29.632	27.291 (0.102)	25.572 (0.138)
S22	3 ^h 22 ^m 05 ^s .39179	-15° 23' 14." 0298	>28.809	29.135 (0.235)	27.219 (0.100)	25.685 (0.161)
S23	3 ^h 22 ^m 05 ^s .43718	-15° 23' 15." 6194	28.340 (0.241)	29.474 (0.331)	>28.665	>26.633
S24	3 ^h 22 ^m 05 ^s .35072	-15° 23' 15." 6022	>28.835	28.097 (0.089)	26.975 (0.078)	25.936 (0.202)
S25	3 ^h 22 ^m 05 ^s .38396	-15° 23' 13." 9958	28.367 (0.230)	28.382 (0.119)	26.046 (0.035)	24.549 (0.057)
S26	3 ^h 22 ^m 05 ^s .33025	-15° 23' 15." 0438	27.518 (0.109)	27.466 (0.055)	26.284 (0.048)	25.134 (0.094)
S27	3 ^h 22 ^m 05 ^s .46232	-15° 23' 14." 9126	>28.841	28.581 (0.137)	27.093 (0.084)	25.445 (0.126)
S28	3 ^h 22 ^m 05 ^s .39871	-15° 23' 13." 9614	>28.808	28.522 (0.132)	27.052 (0.084)	25.443 (0.137)
S29	3 ^h 22 ^m 05 ^s .39210	-15° 23' 13." 9558	>28.908	28.386 (0.117)	28.395 (0.288)	26.075 (0.241)
S30	3 ^h 22 ^m 05 ^s .40792	-15° 23' 13." 8970	>28.952	28.692 (0.154)	27.315 (0.102)	25.459 (0.135)
S31	3 ^h 22 ^m 05 ^s .32555	-15° 23' 14." 6310	>28.961	>29.657	28.039 (0.201)	25.475 (0.127)
S32	3 ^h 22 ^m 05 ^s .32419	-15° 23' 15." 2534	27.612 (0.122)	27.707 (0.062)	27.701 (0.150)	>26.591
S33	3 ^h 22 ^m 05 ^s .37008	-15° 23' 15." 9726	28.700 (0.320)	28.055 (0.088)	28.035 (0.206)	>26.599
S34	3 ^h 22 ^m 05 ^s .42642	-15° 23' 15." 9482	27.164 (0.086)	27.302 (0.045)	26.856 (0.072)	>26.520
S35	3 ^h 22 ^m 05 ^s .38581	-15° 23' 16." 0310	28.710 (0.329)	27.696 (0.062)	28.152 (0.227)	>26.624
S36	3 ^h 22 ^m 05 ^s .34751	-15° 23' 15." 8186	>28.843	>29.672	27.447 (0.120)	25.444 (0.127)
S37	3 ^h 22 ^m 05 ^s .47012	-15° 23' 15." 2990	26.530 (0.051)	26.607 (0.024)	26.564 (0.053)	25.154 (0.095)
S38	3 ^h 22 ^m 05 ^s .35077	-15° 23' 13." 9774	>28.916	>29.672	27.501 (0.123)	25.776 (0.173)
S39	3 ^h 22 ^m 05 ^s .38399	-15° 23' 13." 7882	>28.831	27.847 (0.069)	27.555 (0.138)	25.455 (0.123)
S40	3 ^h 22 ^m 05 ^s .42445	-15° 23' 16." 0202	>28.775	27.545 (0.057)	26.175 (0.040)	24.407 (0.050)
S41	3 ^h 22 ^m 05 ^s .33343	-15° 23' 14." 1682	26.522 (0.049)	26.491 (0.022)	26.209 (0.041)	25.470 (0.128)
S42	3 ^h 22 ^m 05 ^s .31449	-15° 23' 15." 0958	28.411 (0.246)	29.178 (0.236)	>28.665	>26.583

Extended Data Table 2 | Photometric variability of the SN 2012Z progenitor system S1. The 1σ photometric uncertainties are given in parentheses. No corrections for Galactic or host extinction are made here.

Date (UT)	MJD	Exposure (sec)	Counts (e^-)	F555W (mag)
2005-08-06	53588.7	2400	171 (71)	28.36 (0.45)
2005-08-17	53600.0	2400	656 (75)	26.94 (0.13)
2005-08-24	53606.8	2400	282 (67)	27.79 (0.26)
2005-08-27	53610.0	2400	392 (64)	27.49 (0.18)
2005-09-02	53615.6	2400	389 (69)	27.48 (0.19)
2005-09-03	53617.0	2400	308 (66)	27.77 (0.23)
2005-09-05	53618.6	2400	392 (71)	27.49 (0.20)
2005-09-07	53621.0	2400	329 (66)	27.66 (0.22)
2005-09-11	53624.0	2400	429 (68)	27.37 (0.17)
2005-09-16	53629.8	2400	242 (67)	27.98 (0.30)
2005-09-20	53633.4	2400	327 (64)	27.70 (0.21)
2005-09-27	53640.5	2400	193 (66)	28.25 (0.37)
2006-10-24	54032.6	2080	388 (76)	27.26 (0.21)
2006-10-07	54015.3	2080	264 (75)	27.62 (0.31)